Catalysis Today xxx (2015) xxx–xxx

Contents lists available at ScienceDirect

Catalysis Today

journal homepage: www.elsevier.com/locate/cattod

Degradation of β-O-4 model lignin species by vanadium Schiff-base catalysts: Influence of catalyst structure and reaction conditions on activity and selectivity

Heather J. Parker[a,b], Christopher J. Chuck[c], Timothy Woodman[a], Matthew D. Jones[a,*]

[a] Department of Chemistry, University of Bath, Claverton Down, Bath BA2 7AY, UK
[b] Doctoral Training Centre, Centre for Sustainable Chemical Technologies, University of Bath, Claverton Down, Bath BA2 7AY, UK
[c] Department of Chemical Engineering, University of Bath, Claverton Down, Bath BA2 7AY, UK

ARTICLE INFO

Article history:
Received 5 June 2015
Received in revised form 25 August 2015
Accepted 31 August 2015
Available online xxx

Keywords:
Lignin depolymerization
Vanadium
Homogeneous catalysis
Model compound

ABSTRACT

In the pursuit of value-added products from the degradation of the abundant aromatic biopolymer lignin, homogeneous catalysis has the potential to provide a mild, selective route to monomeric phenols. Homogeneous vanadium catalysts have previously been shown to effectively cleave dimeric β-O-4 model lignin compounds, with selectivity for C—C or C—O cleavage, or benzylic oxidation, depending on the ligand structure and oxidation state of the metal. In this study, a systematic kinetic investigation was undertaken in order to gain further understanding of the role of ligand structure and reaction conditions on the activity of vanadium Schiff-base catalysts towards a non-phenolic β-O-4 model lignin dimer, and the selectivity of these species towards C—O bond cleavage. Catalytic activity was found to be increased by the addition of bulky, alkyl substituents at the 3′-position of the phenolate ring, whereas electron-withdrawing substituents were found to dramatically reduce activity irrespective of their size. Selective depolymerization of a phenolic β-O-4 dimer was also achieved.

1. Introduction

The valorization of lignin is widely recognized as an important contributor to the economic viability of the biorefinery concept; despite this lignin is not currently widely exploited as a bioresource, largely due to its recalcitrant nature and resistance to degradation [1–4]. In its native polymeric form lignin is of little commercial value and is routinely burnt to recover process heat, for instance in the paper and pulping industry [1]. It is, however, the most abundant source of renewable aromatic functionality available and effective lignin depolymerization could provide a sustainable route to potentially valuable monomeric phenolic species. Substituted phenolic species obtainable from lignin, such as vanillin, have potential applications as antioxidants [5].

Thermochemical techniques such as pyrolysis and gasification have been employed in the degradation of lignin and have been carried out on both isolated lignin and whole biomass. These processes result in unselective degradation, often partially or fully destroying the intrinsic aromatic structure of the lignin polymer, and complex product mixtures are formed which generally require further upgrading and/or separation to produce higher value products [1,6–8].

In order to selectively obtain valuable aromatic products from lignin, a milder and more elegant deconstruction technique is required; homogeneous catalysts could be employed to improve selectivity whilst potentially avoiding the need for harsh reaction conditions.[2,9,10] The inherent diversity of organometallic complexes allows catalytic activity and selectivity to be tuned, for example to target specific linkages or to produce particular products. Homogeneous species are less likely than their heterogeneous counterparts to promote over-reduction resulting in a loss of aromaticity and are potentially capable of accessing linkages within the three-dimensional structure of the lignin polymer which would be beyond the reach of a traditional heterogeneous catalyst [10].

Most examples of homogeneous lignin depolymerization catalysis to date have been demonstrated solely on model lignin compounds [2]. The relative simplicity of these species compared to native lignin increases the ease of analysis, thereby facilitating mechanistic understanding of the degradation. Whilst a diverse library of model compounds is available, the most common are dimeric compounds containing the β-aryl ether (β-O-4) linkage; as well as being the most abundant linkage in lignin, it is also

* Corresponding author.
E-mail address: mj205@bath.ac.uk (M.D. Jones).

http://dx.doi.org/10.1016/j.cattod.2015.08.045
0920-5861/

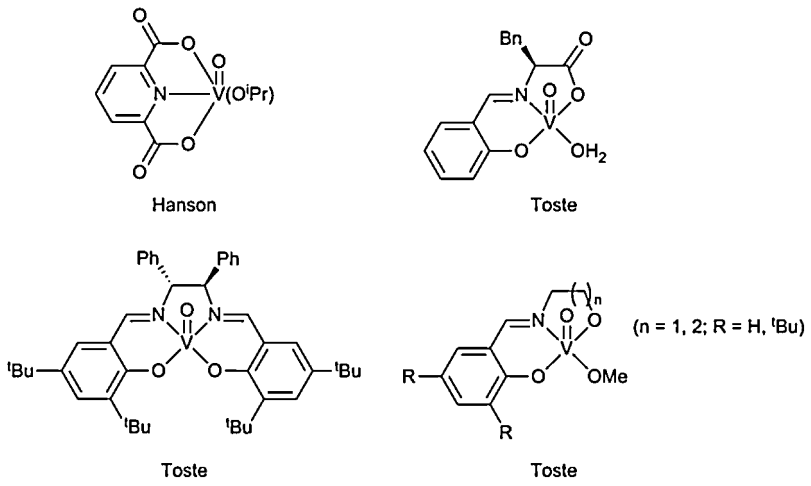

Fig. 1. Representative structures of vanadium-based lignin depolymerization catalysts reported by Hanson [17] and Toste [18].

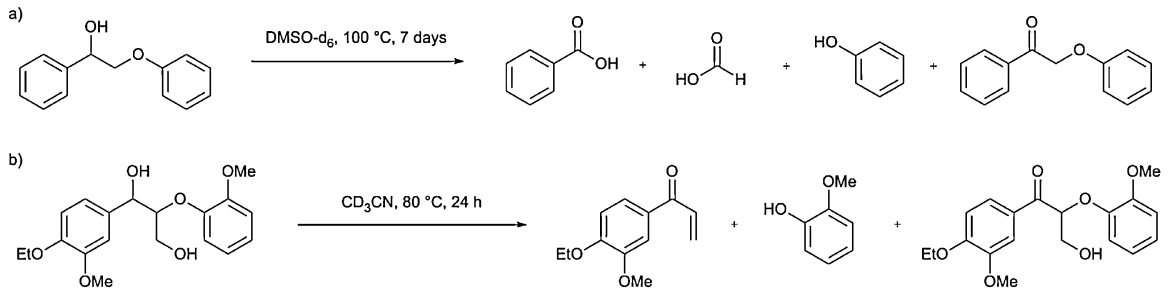

Fig. 2. Degradation of β-O-4 model lignin compounds by vanadium catalysts (a) C—C cleavage and benzylic oxidation, Hanson [17]; (b) C—O cleavage and benzylic oxidation, Toste [18].

amongst the most susceptible to cleavage and therefore represents a desirable target for depolymerization [11].

A wide range of metal complexes have been shown to effectively cleave β-O-4 model lignin compounds [12–16]. For the production of monomeric phenols, vanadium(V) complexes with O/N donor ligands are amongst the most promising homogeneous catalysts, Fig. 1 [17–20]. Changing the ligand structure has been shown to dramatically affect the selectivity of the vanadium complexes towards C—O or C—C bond cleavage, or benzylic oxidation. Hanson et al. reported the C—C bond cleavage in β-O-4 models by dipicolinate vanadium(V) using air as the oxidant. Degradation occurred *via* benzylic oxidation to the oxidation product (OP) followed by subsequent C—C cleavage to form benzoic acid, phenol and formic acid, Fig. 2(a) [17].

Son and Toste reported the depolymerization of a dimeric β-O-4 model compound in the presence of a variety of oxo-vanadium(IV) and (V) species, Fig. 2(b). The former were observed to significantly favour benzylic oxidation to form the oxidation product (OP), over the desired C—O bond cleavage to form the phenol (in this case guaiacol) [18]. The highest selectivity of the vanadium(IV) catalysts for C—O cleavage was 25% in the case of the tridentate ligand.

For the vanadium(V) Schiff-base species, the ligand backbone and functionalization were found to be very important for tuning the activity and selectivity towards C—O bond cleavage over oxidation. Selectivity for C—O cleavage could be improved by extending carbon backbone of the tridentate Schiff-base ligands (from $n = 1$ to $n = 2$, Fig. 1), thereby decreasing the O–V–N bite angle. Both activity and selectivity for C—O cleavage were favoured by the addition of *tert*-butyl substituents at the 3- and 5-positions of the phenolate ring.

The mechanism for C—O bond cleavage was proposed to proceed *via* a formally non-oxidative one-electron V(V)–V(IV) redox process, with the model compound coordinating to vanadium through the benzylic hydroxyl group. Subsequent studies by this group demonstrated the partial depolymerization of Organosolv lignin derived from *Miscanthus giganteus* using vanadium catalysts [21].

In this current study, the role of the Schiff-base ligand on both the activity and selectivity of homogeneous vanadium catalysts was further probed *via* a systematic synthetic and kinetic investigation in order to inform the development of an improved catalytic system.

2. Experimental

2.1. Materials and methods

Where preparative details are not provided, reagents were purchased from Sigma Aldrich, TCI Chemicals, Fluka, Lancaster, Acros Organics or Alfa Aesar and used without additional purification.

NMR spectroscopy: NMR spectra were obtained on one of Bruker Advance 300, 400 or 500 MHz spectrometers at 298 K in $(CD_3)_2SO$, CD_3OD or $CDCl_3$ as solvent. Chemical shifts are reported in parts per million (ppm) relative to the residual solvent peak and coupling constants are reported in Hertz (Hz).

ESI-MS: ESI-MS analysis was recorded on a Bruker Daltonic micrOTOF electrospray time-of-flight (ESI-TOF) mass spectrometer coupled to an Agilent 1200 LC system as an autosampler. 10 μL of sample was injected into a 30:70 flow of water:acetonitrile at 0.3 mL/min into the mass spectrometer.

Elemental analysis: Elemental compositions were obtained by Mr Stephen Boyer at the Microanalysis Service, London Metropolitan University, UK.

Please cite this article in press as: H.J. Parker, et al., Degradation of β-O-4 model lignin species by vanadium Schiff-base catalysts: Influence of catalyst structure and reaction conditions on activity and selectivity, Catal. Today (2015), http://dx.doi.org/10.1016/j.cattod.2015.08.045

X-ray crystallography: All data were collected on a Nonius kappa CCD diffractometer with MoKα radiation (λ = 0.71073 Å). T = 150(2) K throughout and all structures were solved by direct methods and refined on F2 data using the SHELXL-97 suite of programmes.[22] Hydrogen atoms, were included in idealized positions and refined using the riding model. The crystal data is straightforward and the following CCDC numbers 1404037-1404041 contain the information.

2.2. ^{1}H NMR depolymerization studies

2-Phenoxy-1-phenylethanol (33 mg, 0.15 mmol), catalyst (0.5–7 mol%) and hexamethylbenzene (internal standard, 2 mg, 0.01 mmol) were dissolved in 1 mL DMSO-d_6 in an NMR tube (uncapped) and heated (70–120 °C) for 4 days.

2.3. Synthetic procedures

2.3.1. Non-phenolic model compound synthesis

2-Phenoxy-1-phenylethanone: To a solution of 2-bromo-1-phenylethanone (9 g, 45 mmol) in dimethylformamide (150 mL) was added phenol (5 g, 53 mmol) and K_2CO_3 (7.3 g, 53 mmol). The solution was stirred overnight and a colour change from yellow to orange was observed. The reaction mixture was then poured into warm water and left to recrystallize. The crystals were filtered and redissolved in toluene; this solution was dried over $MgSO_4$, filtered and the solvent removed *in vacuo* to give the product as a cream solid in 83% yield. ^{1}H NMR ($CDCl_3$, 300 MHz): δ 5.29 (s, 2H, C$\underline{H}_2$), 6.92–7.06 (m, 3H, Ar-$\underline{H}$), 7.28–7.35 (m, 2H, Ar-$\underline{H}$), 7.48–7.56 (m, 2H, Ar-$\underline{H}$), 7.60–7.68 (m, 1H, Ar-$\underline{H}$), 7.98–8.08 (m, 2H, Ar-$\underline{H}$). ^{13}C{^{1}H} NMR ($CDCl_3$, 75 MHz): δ 70.8, 114.8, 121.7, 128.2, 128.9, 129.6, 133.9, 158.0, 194.6. ESI-MS: m/z calcd for $[C_{14}H_{12}O_2Na]^+$: 235.0735; found: 235.0792.

2-Phenoxy-1-phenylethanol: To a solution of 2-phenoxy-1-phenylethanone (7 g, 33 mmol) in methanol (200 mL) was added $NaBH_4$ (2.5 g, 66 mmol) portion wise. The reaction was stirred for 3 h, after which time the solvent was removed *in vacuo*. The residue was redissolved in ethyl acetate (50 mL) and the reaction was quenched by the addition of aqueous HCl (50 mL). The resulting solution was filtered to remove insoluble salts and the product was extracted into ethyl acetate (3× 20 mL), washed with brine (1× 30 mL), dried over $MgSO_4$ and the solvent removed *in vacuo* to afford a waxy, cream solid in 91% yield. ^{1}H NMR ($CDCl_3$, 300 MHz): δ 4.02 (dd, J = 9.8, 9.0 Hz, 1H, C$\underline{H}_2$), 4.13 (dd, J = 9.8, 3.4 Hz, 1H, C$\underline{H}_2$), 5.15 (dd, J = 8.9, 3.2 Hz, 1H, C$\underline{H}$), 6.91–7.02 (m, 3H, Ar-$\underline{H}$), 7.27–7.51 (m, 7H, Ar-$\underline{H}$). ^{13}C{^{1}H} NMR ($CDCl_3$, 75 MHz): δ 72.6, 73.3, 114.6, 126.3, 128.3, 128.6, 129.6, 144.5, 158.4. ESI-MS: m/z calcd for $[C_{14}H_{14}O_2Na]^+$: 237.0891; found: 237.0894. Elemental Analysis: Anal. Calcd for $C_{14}H_{14}O_2$: C, 78.48; H, 6.59. Found: C, 78.31; H, 6.49.

2.3.2. Bulky alcohol and salicylaldehyde synthesis [23]

2-Trityl-4-methylphenol: *p*-Cresol (25 g, 0.2 mmol) was heated to 100 °C under a flow of argon. Sodium metal (1.1 g, 0.05 mmol) was added slowly with vigorous stirring to form a cresolate melt. To this was added triphenylchloromethane (10.0 g, 0.036 mmol) and the mixture was heated at 140 °C for 3 h. The reaction mixture was cooled to room temperature and subsequently treated with 7% aq. NaOH (100 mL) and ether (100 mL). The organic layer was separated, washed with 7% aq. NaOH (5× 50 mL), water (100 mL), and brine (50 mL), dried over $MgSO_4$ and the solvent removed *in vacuo*. The resulting solid was recrystallized from hot diethyl ether to afford the product as a creamy solid in 46% yield. ^{1}H NMR: (400 MHz, $CDCl_3$) δ 2.19 (s, 3H, C$\underline{H}_3$), 4.33 (s, 1H, O$\underline{H}$), 6.74 (d, J = 8.0 Hz, 1H, Ar-$\underline{H}$), 6.86 (d, J = 2.3 Hz, 1H, Ar-$\underline{H}$), 7.04 (dd, J = 8.0, 2.3 Hz, 1H, Ar-$\underline{H}$), 7.16–7.34 (m, 15H, Ar-$\underline{H}$). ^{13}C{^{1}H} NMR: (100 MHz, $CDCl_3$) δ 20.9, 62.6, 117.9, 126.7, 127.9, 129.2, 129.4, 130.9, 131.0, 132.8, 144.2, 152.2.

3-Trityl-5-methylsalicylaldehyde: 2-Trityl-4-methylphenol (3.5 g, 0.01 mol), hexamethylenetetramine (2.80 g, 0.02 mol) and trifluoroacetic acid (10 mL) were stirred together for 4 h at 120 °C. The mixture was cooled to 80 °C, 33% aq. H_2SO_4 (15 mL) was added and the reaction was heated for a further 2 h at 130 °C. After cooling to room temperature, ethyl acetate (20 mL) and water (30 mL) were added. The organic layer was separated and the water layer extracted with ethyl acetate (3× 20 mL). The combined organic extracts were washed with water (50 mL) and brine (30 mL) and dried over $MgSO_4$. The solvent was removed *in vacuo* and the residue was washed with diethyl ether to yield the product as a pale yellow powder in 49% yield. ^{1}H NMR: (400 MHz, $CDCl_3$) δ 2.26 (s, 3H, C$\underline{H}_3$), 7.10–7.25 (m, 15H, Ar-$\underline{H}$), 7.27–7.30 (m, 1H, Ar-$\underline{H}$), 7.36 (d, J = 2.0 Hz, 1H, Ar-$\underline{H}$), 9.80 (s, 1H, C$\underline{H}$O), 11.11 (d, J = 0.5 Hz, 1H, O$\underline{H}$). ^{13}C{^{1}H} NMR (100 MHz, $CDCl_3$): δ 20.7, 62.9, 120.6, 125.7, 127.2, 127.8, 128.0, 128.2, 129.4, 130.8, 130.9, 132.7, 135.4, 138.8, 144.8, 158.5, 196.5.

3-(1-Adamantyl)-5-methylsalicylaldehyde: 2-(1-Adamantyl)-4-methylphenol (1.0 g, 4.1 mmol), hexamethylenetetramine (1.16 g, 8.3 mmol) and trifluoroacetic acid (7 mL) were stirred together for 4 h at 120 °C. The mixture was cooled to 80 °C, 33% aq. H_2SO_4 (70 mL) was added and the reaction was heated for a further hour at 130 °C. After cooling to room temperature, ethyl acetate (20 mL) and water (30 mL) were added. The organic layer was separated and the water layer extracted with ethyl acetate (3× 20 mL). The combined organic extracts were washed with water (50 mL) and brine (30 mL) and dried over $MgSO_4$. The solvent was removed *in vacuo* and the residue was washed with diethyl ether to yield the product as a pale yellow powder in 66% yield. ^{1}H NMR: (400 MHz, $CDCl_3$) δ 1.74–1.82 (m, 6H, Ad-$\underline{H}$), 2.05–2.10 (m, 3H, Ad-$\underline{H}$), 2.11–2.18 (m, 6H, Ad-$\underline{H}$), 2.31 (s, 3H, C$\underline{H}_3$), 7.13–7.19 (m, 1H, Ar-$\underline{H}$), 7.27 (d, J = 2.3 Hz, 1H, Ar-$\underline{H}$), 9.81 (s, 1H, O$\underline{H}$), 11.64 (s, 1H, C$\underline{H}$O). ^{13}C{^{1}H} NMR: ($CDCl_3$, 75 MHz): δ 20.6, 28.9, 37.0, 40.1, 120.3, 128.2, 131.3, 135.5, 159.4, 197.2.

2.3.3. Ligand synthesis

General procedure: To a solution of the aldehyde (1 g) in methanol (70 mL) was added Na_2SO_4 (8 eq.) and 3-amino-1-propanol (1 eq.), the reaction was heated to reflux and stirred overnight. The mixture was then cooled to room temperature, filtered and concentrated *in vacuo* to afford the product.

***N*-(3-Hydroxypropyl)-3,5-di-chlorosalicylaldimine:** (**1**H$_2$) ^{1}H NMR: ($CDCl_3$, 300 MHz): δ 1.96 (quin, J = 6.3 Hz, 2H, C$\underline{H}_2$), 3.78 (t, J = 6.0 Hz, 2H, C$\underline{H}_2$-OH), 3.77 (t, J = 5.7 Hz, 2H, N-C$\underline{H}_2$), 7.11 (d, J = 2.6 Hz, 1H, Ar-$\underline{H}$), 7.40 (d, J = 2.6 Hz, 1H, Ar-$\underline{H}$), 8.22 (s, 1H, N = C$\underline{H}$). ^{13}C{^{1}H} NMR: ($CDCl_3$, 75 MHz): δ 32.7, 53.9, 59.6, 118.4, 121.3, 123.9, 129.1, 132.8, 159.9, 163.9. ESI-MS: m/z calcd for $[C_{10}H_{12}Cl_2NO_2]^+$: 248.0245; found: 248.0237.

***N*-(3-Hydroxypropyl)-3,5-di-bromosalicylaldimine:** (**2**H$_2$) ^{1}H NMR: ($CDCl_3$, 300 MHz): δ 1.98 (quin, J = 6.3 Hz, 2H, C$\underline{H}_2$), 3.75–3.82 (m, 4H, C$\underline{H}_2$-OH, N-C$\underline{H}_2$), 7.32 (d, J = 2.3 Hz, 1H, Ar-$\underline{H}$), 7.71 (d, J = 2.3 Hz, 1H, Ar-$\underline{H}$), 8.23 (s, 1H, N = CH). ^{13}C{^{1}H} NMR: ($CDCl_3$, 75 MHz): δ 32.7, 53.7, 59.5, 108.0, 113.9, 118.8, 132.9, 138.3, 161.0, 163.8. ESI-MS: m/z calcd for $[C_{10}H_{12}Br_2NO_2]^+$: 337.9209; found: 337.9527.

***N*-(3-Hydroxypropyl)-3,5-di-iodosalicylaldimine:** (**3**H$_2$) ^{1}H NMR: ($CDCl_3$, 300 MHz): δ 1.98 (quin, J = 6.4 Hz, 2H, C$\underline{H}_2$), 3.75–3.80 (m, 4H, C$\underline{H}_2$-OH, N-C$\underline{H}_2$), 7.49 (d, J = 2.3 Hz, 1H, Ar-$\underline{H}$), 8.05 (d, J = 2.3 Hz, 1H, Ar-$\underline{H}$), 8.13 (t, J = 1.0 Hz, 1H, N = C$\underline{H}$). ^{13}C{^{1}H} NMR: ($CDCl_3$, 75 MHz): δ 32.7, 53.5, 59.6, 90.1, 118.8, 140.0, 149.1, 163.5. ESI-MS: m/z calcd for $[C_{10}H_{12}I_2NO_2]^+$: 431.8957; found: 431.8967.

***N*-(3-Hydroxypropyl)-salicylaldimine:** (**4**H$_2$) ^{1}H NMR: ($CDCl_3$, 300 MHz): δ 2.01 (quin, J = 6.4 Hz, 2H, C$\underline{H}_2$), 3.77 (t, J = 6.7 Hz, 2H, C$\underline{H}_2$), 3.81 (t, J = 6.2 Hz, 2H, C$\underline{H}_2$), 6.92 (t, J = 7.5 Hz, 1H, Ar-$\underline{H}$), 7.00

Please cite this article in press as: H.J. Parker, et al., Degradation of β-O-4 model lignin species by vanadium Schiff-base catalysts: Influence of catalyst structure and reaction conditions on activity and selectivity, Catal. Today (2015), http://dx.doi.org/10.1016/j.cattod.2015.08.045

(d, J = 8.3 Hz, 1H, Ar-H), 7.29 (dd, J = 7.7, 1.4 Hz, 1H, Ar-H), 7.32–7.38 (m, 1H, Ar-H), 8.42 (s, 1H, N = CH). $^{13}C\{^1H\}$ NMR: ($CDCl_3$, 75 MHz): δ 33.5, 55.8, 60.2, 117.1, 118.5, 131.3, 132.3, 161.4, 165.3. ESI-MS: m/z calcd for $[C_{10}H_{14}NO_2]^+$: 180.1025; found: 180.1025.

***N*-(3-Hydroxypropyl)-3,5-di-*tert*-butylsalicylaldimine:** (**5**H_2) ^1H NMR: ($CDCl_3$, 250 MHz): δ 1.32 (s, 9H, CH_3), 1.45 (s, 9H, CH_3), 1.98 (quin, J = 6.3 Hz, 2H, CH_2), 3.72 (td, J = 6.6, 1.3 Hz, 2H, N-CH_2), 3.79 (t, J = 6.3 Hz, 2H, CH_2-OH), 7.10 (d, J = 2.5 Hz, 1H, Ar-H), 7.39 (d, J = 2.5 Hz, 1H, Ar-H), 8.40 (t, J = 1.3 Hz, 1H, N = CH), 13.82 (br. s, 1H, Ar-OH). $^{13}C\{^1H\}$ NMR: ($CDCl_3$, 75 MHz): δ 29.4, 31.5, 33.5, 34.2, 35.1, 55.9, 60.3, 117.8, 125.8, 126.9, 136.7, 140.0, 158.2, 166.4. ESI-MS: m/z calcd for $[C_{18}H_{28}NO_2]^-$: 290.2120; found: 290.2121.

***N*-(3-Hydroxypropyl)-3-(1-adamantyl)-5-methylsalicylaldimine:** (**6**H_2) ^1H NMR: (CD_3OD, 300 MHz): δ 1.85–1.91 (m, 6H, Ad-H), 1.99 (quin, J = 6.7 Hz, 2H, CH_2), 2.09–2.16 (m, 3H, Ad-H), 2.22–2.27 (m, 6H, Ad-H), 2.32 (s, 3H, CH_3), 3.75 (t, J = 6.4 Hz, 4H, CH_2-OH, N-CH_2), 7.02 (d, J = 1.3 Hz, 1H, Ar-H), 7.11 (d, J = 1.8 Hz, 1H, Ar-H), 8.46 (s, 1H, N = CH). $^{13}C\{^1H\}$ NMR: (CD_3OD, 75 MHz): δ 20.9, 30.7, 35.0, 38.1, 38.4, 41.6, 56.9, 60.5, 120.0, 128.0, 130.7, 131.3, 138.4, 159.7, 167.9. ESI-MS: m/z calcd for $[C_{21}H_{29}NO_2Na]^+$: 350.2096; found: 350.2089.

***N*-(3-Hydroxypropyl)-3-trityl-5-methylsalicylaldimine:** (**7**H_2) ^1H NMR: (DMSO-d_6, 400 MHz): δ 1.71 (quin, J = 6.6 Hz, 2H, CH_2), 2.21 (s, 3H, CH_3), 3.42 (t, J = 6.3 Hz, 4H, CH_2-OH, N-CH_2), 7.06 (d, J = 2.0 Hz, 1H, Ar-H), 7.13–7.21 (m, 9H, Ar-H), 7.23 (d, J = 1.8 Hz, 1H, Ar-H), 7.28 (t, J = 7.3 Hz, 6H, Ar-H), 8.50 (s, 1H, N = CH). $^{13}C\{^1H\}$ NMR: ($CDCl_3$, 75 MHz): δ 20.8, 21.5, 33.3, 55.8, 60.3, 63.2, 118.6, 125.3, 125.5, 126.1, 127.2, 128.3, 129.1, 130.7, 131.1, 134.4, 134.5, 145.6, 158.0. ESI-MS: m/z calcd for $[C_{30}H_{29}NO_2Na]^+$: 458.2096; found: 458.2102.

2.3.4. Catalyst synthesis

General procedure: Catalyst syntheses were conducted using glove box and Schlenk line techniques under an atmosphere of argon. In a glove box, equimolar amounts of the ligand and VO(O^iPr)$_3$ were dissolved separately in anhydrous dichloromethane. The ligand solution was added dropwise to the metal solution and the reaction mixture was stirred for 0.5 h. The solvent was removed *in vacuo* and recrystallization was attempted from hexane, toluene or dichloromethane.

VO(**1**)(O^iPr): Recrystallized from dichloromethane. ^1H NMR ($CDCl_3$, 300 MHz): 1.46 (d, J = 6.0 Hz, 3H, CH-CH_3), 1.55 (d, J = 6.4 Hz, 3H, CH-CH_3), 1.93–2.11 (m, 1H, CH_2), 2.32–2.43 (m, 1H, CH_2), 3.95–4.10 (m, 1H, CH_2), 4.55 (t, J = 12.2 Hz, 1H, CH_2), 4.92 (d, J = 7.9 Hz, 1H, CH_2), 5.65 (t, J = 11.1 Hz, 1H, CH_2), 5.83 (spt, J = 6.8 Hz, 1H, CH-CH_3), 7.22 (d, J = 2.6 Hz, 1H, Ar-H), 7.54 (d, J = 2.3 Hz, 1H, Ar-H), 8.31 (br. s., 1H, N = CH). $^{13}C\{^1H\}$ NMR: ($CDCl_3$, 75 MHz): δ 24.0, 32.6, 63.6, 80.4, 130.3, 134.2, 162.1. ^{51}V NMR ($CDCl_3$, 105 MHz): δ −563.1. Elemental Analysis: Anal. Calcd for $C_{13}H_{16}Cl_2NO_4V$: C, 41.96; H, 4.33; N, 3.76. Found: C, 41.83; H, 4.46; N, 3.84.

VO(**2**)(O^iPr): Recrystallized from dichloromethane. ^1H NMR ($CDCl_3$, 300 MHz): δ 1.39 (d, J = 6.0 Hz, 3H, CH-CH_3), 1.48 (d, J = 6.0 Hz, 3H, CH-CH_3), 1.86–2.04 (m, 1H, CH_2), 2.22–2.35 (m, 1H, CH_2), 3.94 (d, J = 12.4 Hz, 1H, CH_2), 4.47 (t, J = 12.2 Hz, 1H, CH_2), 4.84 (d, J = 9.0 Hz, 1H, CH_2), 5.56 (td, J = 11.2, 2.8 Hz, 1H, CH_2), 5.75–5.88 (m, 1H, CH-CH_3), 7.32 (d, J = 2.3 Hz, 1H, Ar-H), 7.76 (d, J = 2.3 Hz, 1H, Ar-H), 8.20 (br. s., 1H, N = CH). $^{13}C\{^1H\}$ NMR: ($CDCl_3$, 75 MHz): δ 24.2, 32.6, 63.5, 80.5, 109.3, 134.1, 139.7, 162.0. ^{51}V NMR ($CDCl_3$, 105 MHz): δ −563.2. Elemental Analysis: Anal. Calcd for $C_{13}H_{16}Br_2NO_4V$: C, 33.87; H, 3.50; N, 3.04. Found: C, 33.72; H, 3.40; N, 2.98.

VO(**3**)(O^iPr): Recrystallized from toluene. ^1H NMR ($CDCl_3$, 500 MHz): δ 1.50 (d, J = 6.0 Hz, 3H, CH-CH_3), 1.58 (d, J = 6.0 Hz, 3H, CH-CH_3), 2.03 (q, J = 12.3 Hz, 1H, CH_2), 2.35 (d, J = 12.9 Hz, 1H, CH_2), 4.00 (d, J = 12.0 Hz, 1H, CH_2), 4.52 (t, J = 12.6 Hz, 1H, CH_2), 4.90 (d, J = 9.8 Hz, 1H, CH_2), 5.61 (t, J = 10.6 Hz, 1H, CH_2), 5.90–6.03 (m, 1H, CH-CH_3), 7.58 (br. s, 1H, Ar-H), 8.20 (br. s, 2H, Ar-H, N = CH). $^{13}C\{^1H\}$ NMR: ($CDCl_3$, 75 MHz): δ 24.2, 24.5, 25.6, 32.6, 63.4, 78.9, 80.5, 141.4, 150.8, 161.8. ^{51}V NMR ($CDCl_3$, 132 MHz): δ −562.4. Elemental Analysis: Anal. Calcd for $C_{13}H_{16}I_2NO_4V$: C, 28.13; H, 2.91; N, 2.52. Found: C, 28.00; H, 2.79; N, 2.57.

VO(**4**)(O^iPr): ^1H NMR ($CDCl_3$, 300 MHz): δ 1.37 (d, J = 6.4 Hz, 3H, CH-CH_3), 1.43 (d, J = 6.4 Hz, 3H, CH-CH_3), 1.82–1.99 (m, 1H, CH_2), 2.19–2.31 (m, 1H, CH_2), 3.91 (d, J = 12.4 Hz, 1H, CH_2), 4.42 (tt, J = 12.3, 2.2 Hz, 1H, CH_2), 4.74–4.90 (m, 1H, CH_2), 5.40–5.63 (m, 2H, CH_2, CH-CH_3), 6.77–6.86 (m, 1H, Ar-H), 6.89 (d, J = 8.3 Hz, 1H, Ar-H), 7.26 (dd, J = 7.5, 1.9 Hz, 1H, Ar-H), 7.38 (ddd, J = 8.6, 7.1, 1.7 Hz, 1H, Ar-H), 8.29 (br. s., 1H, N-CH). $^{13}C\{^1H\}$ NMR: ($CDCl_3$, 75 MHz): δ 24.1, 32.7, 63.4, 80.1, 83.0, 118.9, 132.8, 134.9, 163.1. ^{51}V NMR ($CDCl_3$, 105 MHz): δ −556.8. Elemental Analysis: Anal. Calcd for $C_{13}H_{18}NO_4V$: C, 51.49; H, 5.98; N, 4.62. Found: C, 51.32; H, 5.84; N, 4.66.

VO(**5**)(O^iPr): ^1H NMR ($CDCl_3$, 300 MHz): δ 1.25 (s, 9H, C(CH_3)$_3$), 1.37–1.43 (m, 15H, C(CH_3)$_3$ (9H), CH(CH_3)$_2$ (6H)), 1.82–1.91 (m, 1H, CH_2), 2.13–2.24 (m, 1H, CH_2), 3.80–3.91 (m, 1H, CH_2), 4.35 (t, J = 11.7 Hz, 1H, CH_2), 4.70–4.85 (m, 1H, CH_2), 5.43 (t, J = 12.4 Hz, 1H, CH_2), 5.63 (spt, J = 6.0 Hz, 1H, CH(CH_3)$_2$), 7.09 (d, J = 2.6 Hz, 1H, Ar-H), 7.46 (d, J = 2.6 Hz, 1H, Ar-H), 8.27 (br. s, 1H, N = CH). $^{13}C\{^1H\}$ NMR ($CDCl_3$, 75 MHz): δ 24.6, 24.9, 25.4, 29.5, 31.5, 32.1, 32.9, 34.2, 35.2, 63.4, 127.0, 129.6, 141.0, 163.8. ^{51}V NMR ($CDCl_3$, 105 MHz): δ −568.8. Elemental Analysis: Anal. Calcd for $C_{21}H_{34}NO_4V$: C, 60.71; H, 8.25; N, 3.37. Found: C, 60.51; H, 8.88; N, 4.10.

VO(**6**)(O^iPr): ^1H NMR ($CDCl_3$, 300 MHz): δ 1.45 (d, J = 6.0 Hz, 3H, CH-CH_3), 1.53 (d, J = 6.0 Hz, 3H, CH-CH_3), 1.76 (d, J = 11.7 Hz, 3H, Ad-H), 1.86 (d, J = 11.7 Hz, 3H, Ad-H), 1.89–2.00 (m, 1H, CH_2), 2.04–2.11 (m, 3H, Ad-H), 2.14–2.22 (m, 6H, Ad-H), 2.22–2.29 (m, 1H, CH_2), 2.32 (s, 3H, CH_3), 3.92 (dt, J = 12.3, 3.5 Hz, 1H, CH_2), 4.43 (tt, J = 12.6, 1.9 Hz, 1H, CH_2), 4.82–4.93 (m, 1H, CH_2), 5.50–5.59 (m, 2H, CH_2, CH-CH_3), 6.99 (d, J = 1.6 Hz, 1H, Ar-H), 7.23 (d, J = 2.2 Hz, 1H, Ar-H), 8.28 (br. s., 1H, N-CH). $^{13}C\{^1H\}$ NMR ($CDCl_3$, 125 MHz): δ 19.7, 23.5, 23.9, 28.1, 31.8, 36.0, 39.2, 62.4, 78.7, 84.1, 118.4, 126.9, 129.4, 132.1, 162.3. ^{51}V NMR ($CDCl_3$, 105 MHz): δ −556.4.

VO(**7**)(O^iPr): ^1H NMR ($CDCl_3$, 500 MHz): δ 1.06 (d, J = 6.0 Hz, 3H, CH-CH_3), 1.26 (d, J = 6.0 Hz, 3H, CH-CH_3), 1.80–1.93 (m, 1H, CH_2), 2.17 (d, J = 13.2 Hz, 1H, CH_2), 2.27 (s, 3H, CH_3), 3.86 (d, J = 11.7 Hz, 1H, CH_2), 4.33 (t, J = 12.0 Hz, 1H, CH_2), 4.66–4.79 (m, 1H, CH-CH_3), 4.88–4.98 (m, 1H, CH_2), 5.33 (t, J = 11.0 Hz, 1H, CH_2), 7.04–7.40 (m, 17H, Ar-H), 8.25 (br. s., 1H, N = CH). $^{13}C\{^1H\}$ NMR ($CDCl_3$, 75 MHz): δ 20.8, 24.1, 24.4, 32.3, 63.5, 79.1, 84.9, 125.3, 127.1, 127.3, 131.1, 132.1, 136.8, 163.3. ^{51}V NMR ($CDCl_3$, 132 MHz): δ −562.6. Elemental Analysis: Anal. Calcd for $C_{33}H_{34}NO_4V$: C, 70.83; H, 6.12; N, 2.50. Found: C, 70.71; H, 6.24; N, 2.57.

3. Results and discussion

3.1. Catalyst synthesis and characterization

Tridentate salen ligands **1**H_2–**7**H_2 were synthesized *via* condensation of the relevant aldehyde with 3-amino-1-propanol. Subsequent reaction of the ligands with vanadium oxytriisopropoxide under an inert atmosphere gave rise to vanadium(V) complexes VO(**1–7**)(O^iPr), Fig. 3. The catalysts were analyzed by ^1H, $^{13}C\{^1H\}$ and ^{51}V NMR spectroscopy, and solid state structures were obtained for several of the species by single-crystal X-ray diffraction.

The complexes were isolated as red crystalline samples in moderate to good yields. For complexes VO(**1–5**)(O^iPr) the solid state structures were determined by single crystal X-ray diffraction, Fig. 4. In the solid state the complexes are dimeric with the aliphatic alcohol bridging between the two vanadium centres. In all cases the vanadium atoms are in pseudo octahedral environments and the metric data are consistent with vanadium(V) complexes, Table 1.

Please cite this article in press as: H.J. Parker, et al., Degradation of β-O-4 model lignin species by vanadium Schiff-base catalysts: Influence of catalyst structure and reaction conditions on activity and selectivity, Catal. Today (2015), http://dx.doi.org/10.1016/j.cattod.2015.08.045

Table 1
Selected bond distances (Å) and angles (°) for complexes VO(**1–5**)(O^{i}Pr).

	VO(**1**)(O^{i}Pr)	VO(**2**)(O^{i}Pr)	VO(**3**)(O^{i}Pr)	VO(**4**)(O^{i}Pr)	VO(**5**)(O^{i}Pr)
V(1)-O(1)	1.781(2)	1.7815(19)	1.781(2)	1.7905(18)	1.7957(11)
V(1)-O(2)	1.8731(18)	1.8757(19)	1.879(2)	1.8867(18)	1.8870(10)
V(1)-O(3)	1.9193(19)	1.9218(19)	1.925(2)	1.8983(19)	1.9011(10)
V(1)-O(4)	1.596(2)	1.5955(19)	1.595(3)	1.6013(17)	1.5954(11)
V(1)-N(1)	2.192(2)	2.196(2)	2.199(3)	2.178(2)	2.1616(13)
N(1)-V(1)-O(1)	172.96(9)	173.26(9)	173.38(12)	173.97(8)	172.37(5)
O(3)-V(1)-O(1)	93.39(9)	93.68(8)	94.29(11)	93.60(9)	94.73(5)

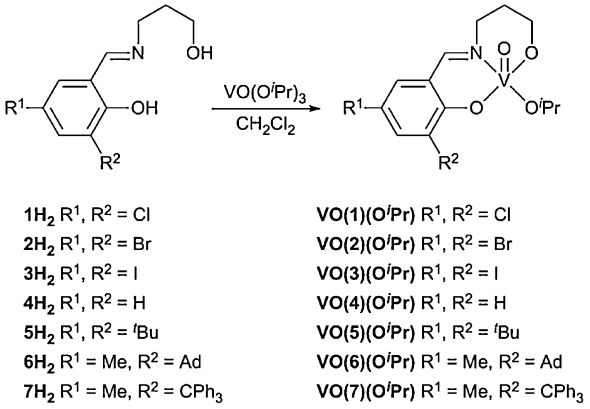

Fig. 3. Synthesis of vanadium Schiff-base catalysts.

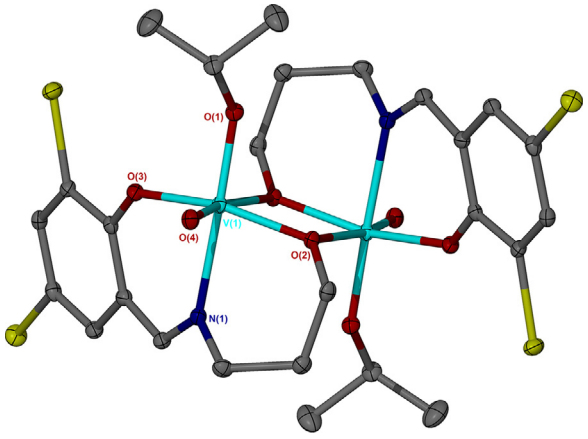

Fig. 4. Solid state structure of VO(**2**)(O^{i}Pr), ellipsoids are shown at the 30% probability level and hydrogen atoms have been removed for clarity.

Interestingly the only previously reported solid state structure of analogous Schiff-base complexes are based on a vanadium-methoxy moieties.[18] In those cases it is observed that the –OMe is bridging (with the H-substituted ligand) or monomeric species (^{t}Bu-substituted ligand) are isolated in the solid-state. However, all examples in this study are dimeric. From ^{1}H solution-state NMR spectroscopic investigations the ligand is "locked" in place as evidenced by the presence of distinct diastereotopic doublets for the CH_2 for the propyl bridge.

To probe the solution state behaviour further, DOSY NMR were obtained for VO(**4,6,7**)(O^{i}Pr) in $CDCl_3$. Measured diffusion constants were found to be 8.4×10^{-1} m^2 s^{-1} (H), 7.8×10^{-10} m^2 s^{-1} (Ad) and 6.8×10^{-10} m^2 s^{-1} (CPh$_3$) respectively. These are consistent with the dimeric solid state structure being maintained in solution. However, when the sample was run in d^8-THF (a coordinating solvent) a significantly more complex NMR spectrum was obtained with two clear species being present in solution, indicating that the dimer is dissociating into a monomer. Thus, in the presence of the coordinating lignin model compound the active catalyst is the monomeric species.

3.2. ^{1}H NMR depolymerization studies

Kinetic investigations in this study were carried out on the non-phenolic model compound 2-phenoxy-1-phenylethanol. Breakdown of the model compound to phenol and acetophenone, and 2-phenoxy-1-phenylethanone (by C—O bond cleavage and benzylic oxidation respectively) was monitored by ^{1}H NMR spectroscopy, Fig. 5 [17]. Conversion of the model compound and yields of acetophenone and 2-phenoxy-1-phenylethanone were quantified by integration of the NMR spectra with respect to an internal standard (hexamethylbenzene). Direct quantification of phenol by this method was not possible due to overlapping resonances, therefore selectivity for C—O bond cleavage was quantified from the yield of co-product, acetophenone.

Both acetophenone and phenol were found to be stable in the presence of the catalyst and did not undergo further reaction. In agreement with previous studies, the benzylic oxidation product (OP), 2-phenoxy-1-phenylethanone, was not broken down under the reaction conditions (results not shown) confirming that degradation occurs directly from the alcohol rather than *via* the OP [18]. This is in contrast to the C—C cleavage reported by Hanson et al. which proceeds *via* oxidation [17]. No conversion of the model compound was observed in the absence of a catalyst.

The overall activity of catalysts VO(**1–7**)(O^{i}Pr) for the conversion of the model compound was investigated and pseudo first order rate constants were determined by monitoring the concentration of the model compound as a function of time, Fig. 6. As steric bulk on the phenolate ring had previously been reported to improve catalyst activity [18], possibly by preventing the aggregation of active catalytic intermediates into inert dimeric species, the size of the substituent at the 3′-position was systematically increased. The unsubstituted catalyst VO(**4**)(O^{i}Pr) was found to have an observed rate constant, k', of 0.24 days^{-1}. As in the literature, a

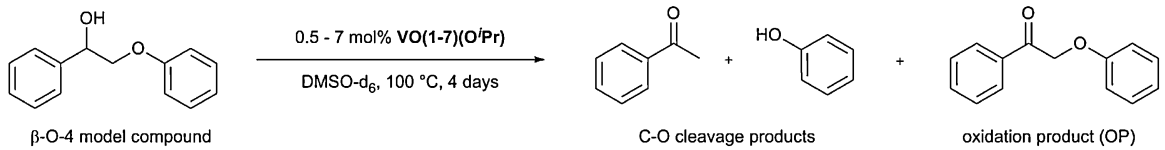

Fig. 5. Degradation of β-O-4 lignin model compound 2-phenoxy-1-phenylethanol to C—O cleavage products acetophenone and phenol, and benzylic oxidation product (OP) 2-phenoxy-1-phenylethanone.

Please cite this article in press as: H.J. Parker, et al., Degradation of β-O-4 model lignin species by vanadium Schiff-base catalysts: Influence of catalyst structure and reaction conditions on activity and selectivity, Catal. Today (2015), http://dx.doi.org/10.1016/j.cattod.2015.08.045

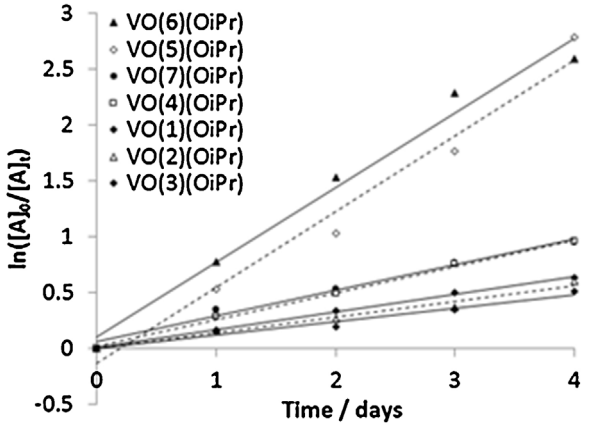

Catalyst	k' / days^{-1}
VO(**1**)(O^{i}Pr)	0.16 ± 0.01
VO(**2**)(O^{i}Pr)	0.14 ± 0.01
VO(**3**)(O^{i}Pr)	0.12 ± 0.01
VO(**4**)(O^{i}Pr)	0.24 ± 0.01
VO(**5**)(O^{i}Pr)	0.68 ± 0.06
VO(**6**)(O^{i}Pr)	0.67 ± 0.05
VO(**7**)(O^{i}Pr)	0.23 ± 0.02

Fig. 6. $\ln([A]_0/[A]_t)$ *vs.* time for VO(**1–7**)(O^{i}Pr), where $[A]_t$ is the concentration of model compound 2-phenoxy-1-phenylethanol (in mol dm^{-3}) at time, t and k' is the pseudo first order rate constant (5 mol% catalyst, DMSO-d_6, 100 °C). {$[A]_0$ = initial concentration of model compound = 0.15 mol dm^{-3}, $[A]_t$ = concentration of model compound at time t as determined from ^{1}H NMR spectroscopic analysis.}

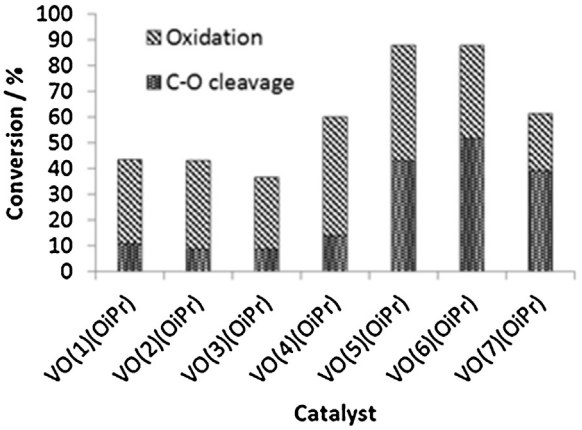

Catalyst	Ratio of C-O Cleavage : Oxidation products
VO(**1**)(O^{i}Pr)	0.34
VO(**2**)(O^{i}Pr)	0.26
VO(**3**)(O^{i}Pr)	0.33
VO(**4**)(O^{i}Pr)	0.30
VO(**5**)(O^{i}Pr)	0.96
VO(**6**)(O^{i}Pr)	1.43
VO(**7**)(O^{i}Pr)	1.80

Fig. 7. Effect of ligand substituents on conversion and selectivity for C—O bond cleavage in the degradation of model compound 2-phenoxy-1-phenylethanol. Conditions: 5 mol% catalyst, DMSO-d_6, 100 °C.

dramatic increase in activity was observed on addition of *tert*-butyl groups at the 3′ and 5′ positions, with $k' = 0.68$ days^{-1} for VO(**5**)(O^{i}Pr). Adamantyl-substitution at the 3′-position produced no further improvement in rate {VO(**6**)(O^{i}Pr): $k' = 0.67$ days^{-1}}, whilst increasing the size of the substituent further again to a trityl group resulted in a significant decrease in activity back to the level of the unsubstituted catalyst {VO(**7**)(O^{i}Pr): $k' = 0.23$ days^{-1}}. If the role of steric bulk in increasing activity is related to the prevention of dimerization, it appears that the *tert*-butyl group is large enough to achieve this. The drop in activity observed with the trityl substituent could be a result of reduced access of the model compound to the catalyst active site.

In order to probe the electronic effects of the ligand on catalyst performance, a range of halogen substituted catalysts were also subjected to investigation. These species were significantly less active than their bulky alkyl-substituted counterparts and there was a very minor decrease in activity with increasing substituent size going down the group ($k' = 0.16$, 0.14, 0.12 days^{-1} for VO(**1–3**)(O^{i}Pr) respectively).

Whilst catalytic activity is important, the selectivity of the catalyst for carbon—oxygen bond cleavage over benzylic oxidation is the priority, as breaking the C—O bonds in lignin is more likely to facilitate depolymerization, Fig. 7. Catalysts VO(**1–3**)(O^{i}Pr) with electron-withdrawing ligand substituents were found to favour oxidation and demonstrated low selectivity towards C—O bond cleavage, whilst selectivities for the alkyl-substituted species VO(**5–7**)(O^{i}Pr) were significantly higher. The unsubstituted catalyst VO(**4**)(O^{i}Pr) displayed an intermediate selectivity. The major difference between the trends in activity and selectivity was in the performance of the three bulky alkyl-substituted species. Selectivity of the catalyst appeared to be directly related to the size of the substituent, with the ratio of C—O cleavage to oxidation increasing as H ≪ ^{t}Bu < Ad < CPh_3, from 0.30 for the unsubstituted catalyst up to 1.80 for the bulkiest trityl substituent. This trend in selectivity could be a result of the increased steric hindrance impeding the access of molecular oxygen to the active site of the catalyst; thus favouring C—O cleavage over C—O oxidation. This signposts towards potential future avenues of research in this field. Analogous investigations using a dipicolinate vanadium(V) catalyst were reported to achieve relatively high selectivity for depolymerization (*via* C—C cleavage) over benzylic oxidation, however activity was lower, with only 95% conversion after 7 days at 10 mol% loading as compared to >95% in under 4 days at 5 mol% loading for VO(**6**)(O^{i}Pr).

Catalytic activity towards conversion of the β-O-4 model lignin compound was found to increase with increasing catalyst loading.

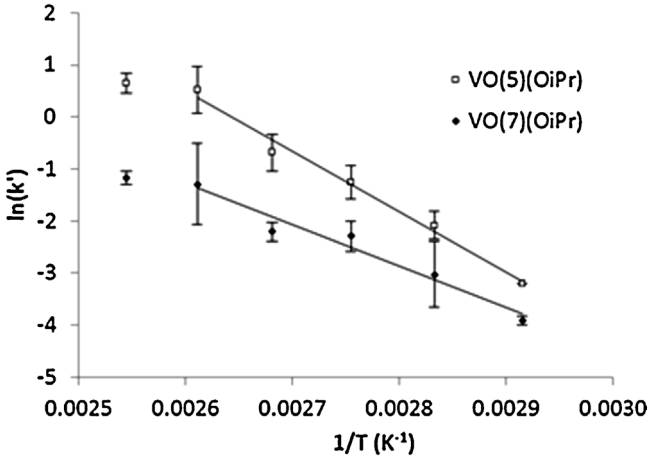

Fig. 8. Arrhenius plots for the degradation of 2-phenoxy-1-phenylethanol by VO(**5,7**)(O^{i}Pr). Conditions: 5 mol% catalyst, DMSO-d_6, 70–120 °C.

Please cite this article in press as: H.J. Parker, et al., Degradation of β-O-4 model lignin species by vanadium Schiff-base catalysts: Influence of catalyst structure and reaction conditions on activity and selectivity, Catal. Today (2015), http://dx.doi.org/10.1016/j.cattod.2015.08.045

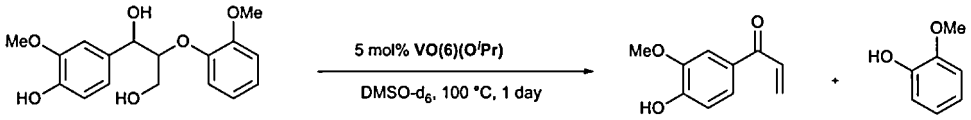

Fig. 9. Depolymerization of phenolic β-O-4 model lignin compound guaiacylglycerol-β-guaiacyl ether.

This effect was seen to tail off above 7 mol%, which could be due to insolubility of the catalyst at higher loadings. It is more likely, however, that it is a result of mass transfer limitations resulting from inefficient mixing in the narrow, unstirred reaction vessel. The selectivity was found to be largely unaffected by changes in the catalyst loading.

The *tert*-butyl and trityl substituted catalysts VO(**5**)(O^{i}Pr) and VO(**7**)(O^{i}Pr) were subjected to further investigation at a range of temperatures. Unsurprisingly, catalyst turnover was found to improve with increasing temperature; more interestingly, however, the selectivity for C—O bond cleavage over oxidation was also significantly enhanced, increasing from 0.88 at 70 °C to 3.73 at 120 °C. This trend was also observed for VO(**5**)(O^{i}Pr), with a rise in C—O cleavage selectivity from 0.51 to 1.89 over the same temperature range. Again, this highlights potential for increasing the selectivity in vanadium-catalyzed systems.

Rate constants for VO(**5**)(O^{i}Pr) and VO(**7**)(O^{i}Pr) as a function of temperature were plotted in a classic Arrhenius form, Fig. 8. From this data, two different regimes were observed; below around 400 K, the rate appears to be limited by the kinetics of the reaction itself, however above this temperature an external influence dominates the kinetics. This is most likely a mass transfer limited regime. Regression analysis of the linear low temperature regime provided values for the activation energy (E_a) for conversion of the β-O-4 model compound; in the case of VO(**4**)(O^{i}Pr) E_a was calculated to be 96 ± 6 kJ mol^{-1}, whilst for VO(**7**)(O^{i}Pr) the value was found to be 66 ± 8 kJ mol^{-1}.

It had previously been noted that oxygen is not required for catalyst turnover, but that activity was reduced under anaerobic conditions [18]. Degradation of the model compound in the presence of VO(**7**)(O^{i}Pr) was investigated under standard and low oxygen concentrations (100 °C, 4 days, uncapped and capped NMR tubes). As expected, a significant reduction in catalytic activity was observed under low oxygen conditions ($k' = 0.23 \pm 0.02$, 0.10 ± 0.02 days^{-1}) for standard and low oxygen respectively). Despite the reduced activity, restricting the availability of oxygen further increased selectivity for C—O bond cleavage to 2.29 (from 1.80 under standard conditions).

To further assess the suitability of these vanadium catalysts for lignin depolymerization, catalyst VO(**6**)(O^{i}Pr) was tested for activity on phenolic β-O-4 model lignin compound guaiacylglycerol-β-guaiacyl ether under analogous conditions, Fig. 9. ^{1}H NMR analysis confirmed complete conversion of the model compound within 24 h and indicated 100% selectivity for C—O bond cleavage, with no evidence of the ketone oxidation product. Products were confirmed by GC–MS. Further work is ongoing to investigate the effect of these catalysts on real lignin substrates.

Our catalyst appears to be more active for the breakdown of this model compared to the previous one utilized in this study. We only observe evidence for C—O cleavage and no evidence for C—C cleavage in agreement with previous studies by Toste and Hanson [18,19].

4. Conclusions

Vanadium Schiff-base complexes have been shown to be effective catalysts for the degradation of both phenolic and non-phenolic β-O-4 model lignin compounds. For the non-phenolic model, kinetic investigations revealed that a subtle balance of steric and electronic effects is responsible for tuning the activity and selectivity of these catalysts towards C—O bond cleavage. The unsubstituted catalyst, VO(**4**)(O^{i}Pr) and those with electron-withdrawing ligand substituents demonstrated low activities and selectivities. Bulky, electron-donating ligand substituents were found to produce the most selective catalysts, with the bulkiest trityl group effecting the highest selectivity. Catalytic activity was also improved by the addition of bulky aliphatic substituents such as *tert*-butyl and adamantyl groups, however the trityl-substituted complex was less active, possibly as a result of increased steric hindrance preventing access of the model compound to the metal centre.

The next step in this work is to assess the applicability of these catalysts to the depolymerization of real lignin substrates. Amongst the major challenges to be overcome in the use of homogeneous catalysts for lignin depolymerization is that of catalyst stability and recyclability, however the potential to achieve highly selective degradation to value-added products makes this a highly interesting avenue of research.

Acknowledgements

We thank the EPSRC for funding (DTC studentship for HJP, Grant EP/G03768X/1). CJC would like to thank Rodger and Sue Whorrod for their generous donation to the University of Bath resulting in the Whorrod Research Fellowship. Data created during this research are openly available from the University of Bath data archive at 10.15125/BATH-00135 (Link: http://dx.doi.org/10.15125/BATH-00135).

References

[1] J.E. Holladay, J.J. Bozell, J.F. White, D. Johnson, Top Value-Added Chemicals from Biomass. Results of Screening for Potential Candidates from Biorefinery Lignin, vol. II, U.S. Department of Energy (DOE) by PNNL, Richland, WA, USA, 2007.
[2] J. Zakzeski, P.C.A. Bruijnincx, A.L. Jongerius, B.M. Weckhuysen, Chem. Rev. 110 (2010) 3552–3599.
[3] M. Kleinert, T. Barth, Energy Fuels 22 (2008) 1371–1379.
[4] A.J. Ragauskas, G.T. Beckham, M.J. Biddy, R. Chandra, F. Chen, M.F. Davis, B.H. Davison, R.A. Dixon, P. Gilna, M. Keller, P. Langan, A.K. Naskar, J.N. Saddler, T.J. Tschaplinski, G.A. Tuskan, C.E. Wyman, Science 344 (2014) 1246843.
[5] A. Tai, T. Sawano, F. Yazama, H. Ito, Biochim. Biophys. Acta 1810 (2011) 170–177.
[6] M.P. Pandey, C.S. Kim, Chem. Eng. Technol. 34 (2011) 29–41.
[7] C. Xu, R.A.D. Arancon, J. Labidi, R. Luque, Chem. Soc. Rev. 43 (2014) 7485–7500.
[8] T. Yoshikawa, T. Yagi, S. Shinohara, T. Fukunaga, Y. Nakasaka, T. Tago, T. Masuda, Fuel Process. Technol. 108 (2013) 69–75.
[9] J.G. de Vries, P.J. Deuss, K. Barta, Catal. Sci. Technol. 4 (2014) 1174–1196.
[10] P.J. Deuss, K. Barta, Coord. Chem. Rev. (2015), http://dx.doi.org/10.1016/j.ccr.2015.02.004.
[11] S. Kim, S.C. Chmely, M.R. Nimlos, Y.J. Bomble, T.D. Foust, R.S. Paton, G.T. Beckham, J. Phys. Chem. Lett. 2 (2011) 2846–2852.
[12] J.M. Nichols, L.M. Bishop, R.G. Bergman, J.A. Ellman, J. Am. Chem. Soc. 132 (2010) 12554–12555.
[13] A. Wu, B.O. Patrick, E. Chung, B.R. James, Dalton Trans. 41 (2012) 11093–11106.
[14] A.G. Sergeev, J.F. Hartwig, Science 332 (2011) 439–443.
[15] M.C. Haibach, N. Lease, A.S. Goldman, Angew. Chem. Int. Ed. 53 (2014) 10160–10163.
[16] R.G. Harms, I.I.E. Markovits, M. Drees, h.c.m.W.A. Herrmann, M. Cokoja, F.E. Kühn, ChemSusChem 7 (2014) 429–434.

Please cite this article in press as: H.J. Parker, et al., Degradation of β-O-4 model lignin species by vanadium Schiff-base catalysts: Influence of catalyst structure and reaction conditions on activity and selectivity, Catal. Today (2015), http://dx.doi.org/10.1016/j.cattod.2015.08.045

[17] S.K. Hanson, R.T. Baker, J.C. Gordon, B.L. Scott, D.L. Thorn, Inorg. Chem. 49 (2010) 5611–5618.
[18] S. Son, F.D. Toste, Angew. Chem. Int. Ed. 49 (2010) 3791–3794.
[19] S.K. Hanson, R.L. Wu, L.A. Silks, Angew. Chem. Int. Ed. 51 (2012) 3410–3413.
[20] B. Sedai, C. Diáz-Urrutia, R.T. Baker, R. Wu, L.A.P. Silks, S.K. Hanson, ACS Catal. 1 (2011) 794–804.
[21] J.M.W. Chan, S. Bauer, H. Sorek, S. Sreekumar, K. Wang, F.D. Toste, ACS Catal. 3 (2013) 1369–1377.
[22] G. Sheldrick, Acta Crystallogr. A 64 (2008) 112–122.
[23] A.I. Kochnev, I.I. Oleynik, I.V. Oleynik, S.S. Ivanchev, G.A. Tolstikov, Russ. Chem. Bull. 56 (2007) 1125–1129.

Please cite this article in press as: H.J. Parker, et al., Degradation of β-O-4 model lignin species by vanadium Schiff-base catalysts: Influence of catalyst structure and reaction conditions on activity and selectivity, Catal. Today (2015), http://dx.doi.org/10.1016/j.cattod.2015.08.045